Head Movement in Normal Subjects During Simulated PET Brain Imaging with and without Head Restraint

Michael V. Green, Jürgen Seidel, Stacey D. Stein, Thomas E. Tedder, Kenneth M. Kempner, Caroline Kertzman and Tom A. Zeffiro

Department of Nuclear Medicine, Clinical Center, Biomedical Engineering and Instrumentation Program, National Center for Research Resources, Computer Systems Laboratory, Division of Computer Research and Technology, Medical Neurology Branch, National Institute of Neurological Disease and Stroke, National Institutes of Health, Bethesda, Maryland

Head movement during brain imaging is recognized as a source of image degradation in PET and most other forms of medical brain imaging. However, little quantitative information is available on the kind and amount of head movement that actually occurs during these studies. We sought to obtain this information by measuring head movement in normal volunteers. **Methods:** Head position data were acquired for 40 min in each of 13 supine subjects with and without head restraint. These data were then used to drive a mathematically simulated head through exactly the same set of movements. The positions of point sources embedded in this head were computed at each location and these data summarized as movement at FWHM in each of the three coordinate directions. **Results:** Head movement increased with the length of the sampling interval for studies of either type (with or without head restraint), but the amount and rate of increase with restraint was much smaller. In contrast, head movement during consecutive, short sampling intervals was small and did not increase with time. Spatial gradients in head movement were detected within each study type, and significant spatial differences in head movement were found between study types. **Conclusions:** Head movements in normal, supine subjects, though small, can cause the effective resolution of a brain imaging study to appear to vary in space and time. These effects can be reduced significantly with head restraint and may also be reduced by dividing the acquisition of a single image into a sequence of short images (instead of a single long image), aligning these images spatially and summing the result.

Key Words: PET; brain imaging; head movement

J Nucl Med 1994; 35:1538–1546

Head movement during tomographic brain imaging studies can degrade image quality (*1,2*) depending on the type and amount of motion executed during the data acquisition period. If these motions are small, random and the same throughout the brain, image degradation may be negligible. If these motions are large, nonrandom and nonhomogeneously spread over the brain, image degradation may be severe. Effects may include artificial spatial gradients in image brightness (or count density) and other subtle distortions which worsen as study length increases. In this study, we sought to measure, characterize and interpret the effect of these movements over periods of time and under environmental conditions similar to those commonly encountered during brain imaging with positron emission tomography (PET).

METHODS

Spatial Tracking System

Figure 1 shows the experimental arrangement for measuring head movement in supine subjects. The spatial tracking system (see Appendix A) consists of four components: (1) a transducer, which is attached to the object whose movement is to be measured (the head); (2) a reference source fixed to the bed whose center is the origin of coordinates for the system; (3) an electronics unit, which manipulates the signals from the transducer to compute the transducer's translational and angular position with respect to the reference source; and (4) a personal computer, which controls the system, acquires the position data generated by the electronics unit, and stores these data as they are generated.

The reference source is an electromagnet that continuously broadcasts a low-frequency alternating magnetic field. A portion of this field is intercepted by three mutually perpendicular conducting coils encased in the transducer housing. The currents induced in these coils by the alternating field depend on the coil's distance and orientation relative to the reference source. Thus, the position and orientation of the transducer relative to the center of the reference source can be calculated from these varying currents. In the experiments described here, the measurement system was set to take one sample of the transducer position and orientation every 2.5 sec. By "sample" we mean one full set of the six coordinate values necessary to describe completely the position and orientation of the transducer in space, and by presumption, the position and orientation of anything to which the transducer is rigidly attached (such as the head). The reference

Received Aug. 19, 1993; revision accepted Apr. 7, 1994.
For correspondence and reprints contact: Michael V. Green, Room 1C401, Building 10, National Institutes of Health, Bethesda, MD 20892.

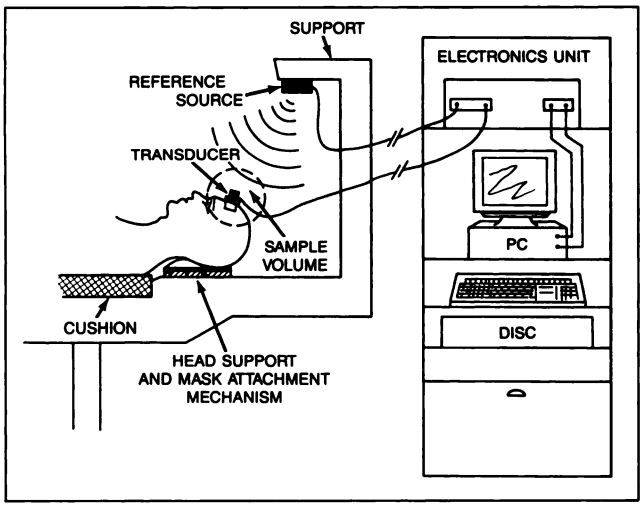

FIGURE 1. Experimental arrangement for measuring head movement in supine subjects.

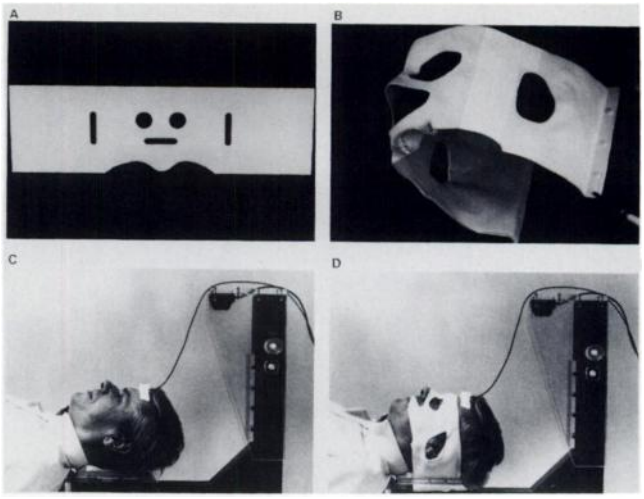

FIGURE 3. Prepunched thermoplastic template before (A), and after (B), molding to a subject's face. Head movement is being monitored without restraint in (C) and with restraint in (D). The reference source (small black box at upper right in C and D), the transducer (attached to the subject's forehead), the head support (under the subject's head) and the mechanism for clamping the mask to the support are visible.

source coordinate system is shown in Figure 2. Three translational coordinates are required to locate the center of the transducer relative to the center of the reference source (X_o, Y_o, and Z_o), and three angular coordinates (Azimuth, Elevation and Roll) are required to depict the angular orientation of the transducer with respect to the reference source coordinate system. When these angles are small (as they are in this study), they may be thought of as independent rotations about each of the fixed coordinate axes: Azimuthal motions can be regarded as rotations of the head about an axis perpendicular to the face; Elevation motions can be regarded as rotations of the head about an axis through the ears; Roll motions can be regarded as rotations of the head about the body long-axis. At the measurement frequency noted above, approximately 1000 of these coordinate samples were collected from each subject in each 40-min session.

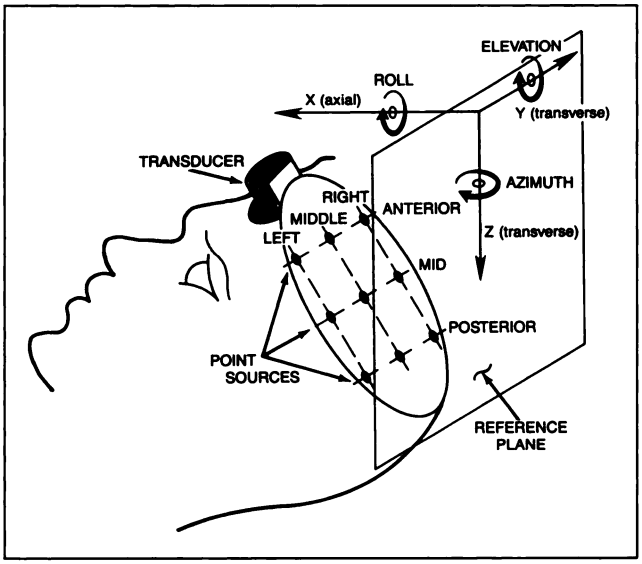

FIGURE 2. Definition of system geometry and point source locations. The transducer is imagined attached to the center of the forehead of the phantom with sources arranged in parallel rows 3 cm, 11.5 cm and 20 cm below the transducer and in three columns, 6.5 cm to the left and 6.5 cm to the right of the transducer, and one directly below the transducer.

Performance of the Spatial Tracking System

The performance of the tracking system was evaluated for each of the six coordinate directions independently by moving the transducer through known angular and translational steps with a precision mechanical drive mechanism fabricated mostly from plastic components. The "true" position or angle of the transducer measured with this device was then compared to the position or angle measured with the spatial tracking system. For each angular coordinate, the transducer was rotated in 0.35-degree steps through the range ± 6.0 degrees. For each translational coordinate, the transducer was moved linearly in 0.7-mm steps through the range ± 7.5 mm. In these tests, the transducer was moved through the same volume of space (the "sample" volume shown in Figure 1) usually occupied by the transducer during human studies and under the same environmental conditions as during these studies (described below).

The resolution and stability of the system were also assessed by fixing the transducer in the sample volume and recording the apparent movement of the motionless transducer during 45 consecutive 40-min intervals (30 hr). These data were then used to calculate corrections that removed the effect of these spurious, machine-induced offsets from the measured source positions.

Attachment of the Transducer to the Head

If transducer movements are to be interpreted as brain movements, the transducer/brain combination must move as a single rigid unit. We assumed that when the transducer was firmly attached to the forehead (Fig. 3), subsequent movements of the transducer represented brain movements. To accomplish this, we cleaned the forehead with alcohol and attached the transducer to the forehead with a 1-inch diameter, double-sided adhesive disc. After firmly pressing the disc to the skin over its full surface area, additional strips of adhesive tape were applied across the top of the transducer to bind the unit to an even larger forehead surface

area. This arrangement appeared to work satisfactorily as long as the subject did not actively contract the facial muscles. Such movements, however, could have gone undetected during the extended data-collection period in each subject. Therefore, we used the following strategy to remove gross skin-movement artifacts from each data record. When subjects voluntarily exercised their facial muscles and visibly moved the transducer on the forehead, the corresponding record of transducer coordinates usually took on a characteristic appearance. Before movement was initiated, the coordinate values were usually stable or slowly drifting in one direction or another. During movement of the facial muscles, one or more coordinate values changed dramatically, usually within one or two 2.5-sec sampling periods. Upon relaxation of the facial muscles, usually in a few seconds, the coordinate values returned in almost every case to nearly the same values exhibited before muscle contraction began. In contrast to this behavior, "real" head movements were usually associated with much slower changes in the coordinate values, with no obvious tendency to return to earlier stable values. Therefore, all six coordinate records for each study were scanned and all samples occurring during an event like that described above, i.e., an abrupt shift from a stable value followed in a few seconds or tens of seconds by a return to nearly the same starting value, were removed from the data record. Out of some 25,000 position and orientation samples taken in this study, only 44 were removed by this criterion. Thus, skin movement artifacts, as defined by our criterion, were not common. These modified data, rather than the raw position data, were analyzed to obtain the values shown in Results.

Creation of the Thermoplastic Face Mask

Half of the measurements were made as the head was restrained by a face mask created from a piece of thermoplastic pre-punched with ear, eye and nose holes (Fig. 3, Appendix B). The sheet is heated in warm water until it becomes soft and pliable, placed over the face, and carefully molded to fit all of the major facial contours (the bridge of the nose, the orbits, cheekbones). A flap of material is also folded into the mouth forming a bite-plate. After molding is complete but before the material hardens, the ends, or "wings", of the mask are clamped to the head support so that the mask and head support form a single unit. When the mask cools to room temperature, it becomes semi-rigid and resists head movement at all contact points.

Environmental Factors

The position measurement system is adversely affected by large metallic objects near the reference source and transducer (see Appendix C). We sought, therefore, to minimize the amount of metal near the head. The table upon which each subject reclined was fabricated by placing metallic supports necessary for rigidity as far from the head as possible. In addition, at the head end of the table, the reference source support (Figs. 1 and 3), the head support, screws, and fixtures were made of either wood or plastic except for two negligibly small metal thumbscrews used to clamp the mask to the tabletop. Before any measurements were made, the head end of the bed was placed near the room center. All nearby objects likely to contain metal were removed from the room or moved as far as possible from the measurement region. In normal operation, the nearest metal to the reference source was more than one meter away (in the table), while the transducer was never further than 40 cm from the source. The other features of the subject bed, the head support, the cushioned pad, the apparatus used to attach the thermoplastic mask to the head support, and the physical layout of these elements, were the same as, or very similar to, those of the patient bed used during actual PET imaging in our laboratory.

Subject Population and General Study Conditions

Thirteen healthy adult volunteers (six females, seven males, mean age 35 yr) comprised the study population. None of the subjects were required to meet any special pre-study conditions or to restrict or alter their normal activities in any way. All subjects were able to recline in the supine position without difficulty. Before each data collection, the subject was made as comfortable as possible by placing a pillow under the knees for support or at other locations suggested by the subject. If the study did not require the thermoplastic mask, the transducer was attached to the forehead. The subject was then told that data collection was about to begin and to remain awake and motionless during the data-collection period. For studies in which the mask was used, the mask was formed to the face and attached to the head support as described above. When the mask had solidified, the transducer was attached to the forehead, and the subject was told to remain awake and motionless. After these instructions, room lighting was reduced to a subdued level and data collection was started. No other interactions with the subject occurred until after data acquisition was completed 40 min later. During data collection the subject was alone in the study room. An observer was stationed just outside the room however, and, at 10-min intervals, unobtrusively watched the subject for several minutes to assess the general level of compliance with the study directions. No obvious departures from these directions, e.g., gross body movements, general agitation, etc., were observed in any of the 26 sessions. All sessions were carried out in the same room at roughly the same time of day (mid-morning) under these same conditions with or without the mask. The study order, mask or no mask, was chosen at random. The alternate study was usually carried out about 1 wk after the first study.

Data Analysis

The transducer position measurements (corrected for superficial skin movement) cannot be directly related to image degradation since the transducer samples movement at only one point outside the brain. This limitation can be overcome with the scheme illustrated in Figure 2. We imagine the transducer to be rigidly attached not only to the forehead, but also to a transverse plane that passes through the brain. On this plane we distribute nine point objects (or point sources) with the spacing and arrangement shown in the figure. A source is located in this three-by-three grid using the included terminology. For example, the point source located directly below the transducer at the back of the brain is called the middle-posterior source.

We now imagine that the source plane is initially coincident with one tomographic scanning plane (the reference plane in the figure) of a perfect tomographic scanner, one with infinitely fine in-plane and axial resolution. As the head moves during data acquisition, the transverse plane containing the transducer and the point sources will rotate and translate, moving these sources to new locations in the scanner coordinate system. Since we know the position of each source in the fixed transverse plane and the orientation and position of this plane with respect to the scanner, we can compute the new position of each source in the scanner coordinate system (see Appendix D). In aggregate, these displacements represent "blurring" of the point sources due to head movement. If no such movement was present, the nine sources would be imaged by the ideal scanner as true points in their correct absolute positions. With head movement, however, the

point objects will appear in adjacent scan planes and will be "smeared out" in-plane. Thus, instead of being imaged as coplanar "dots" in three-dimensional space, the point objects will be imaged as globular clusters of points, the dimensions of which are determined by the magnitude of the motions along the three scanner coordinate axes. Each data set was transformed in this manner to yield the X, Y and Z displacements of each point source in the scanner coordinate system. These data were then summarized by computing the standard deviation of the mean X, Y and Z position of each source for each study. These standard deviation values were then multiplied by the constant 2.35 in order to change the magnitudes of the measured standard deviations to (approximately) the same scale as FWHM usually used to express physical scanner resolution (see Appendix E). Hereafter, we shall refer to these scaled values as "movement FWHM" or simply FWHM. These movement FWHM values were, in turn, corrected for instrument offset errors, also expressed as FWHM, by subtracting mean instrument offset FWHM from the corresponding position mean FWHM using the formula:

$$\text{FWHM (corrected)} = [(\text{measured FWHM})^2 - (\text{transducer stationary FWHM})^2]^{1/2}.$$

The corrected data were summarized for the study population by computing the population mean FWHM and standard error of the population mean for each source in the three coordinate directions. These data portray source movement as a function of source location.

In order to determine how the FWHM values evolved over time, we computed FWHM in two different ways. With the first method, each record of source position was divided into segments of increasing cumulative length, i.e., 0 to 5 min, 0 to 10 min, etc., and FWHM computed for each interval. The FWHM values computed in this way correspond to those that would be observed during imaging studies of increasing length (the usual case). With the second method, the record of source positions was divided into consecutive 5-min intervals, and FWHM was computed for each interval independently. This method corresponds to an imaging study performed as a sequence of short imaging intervals. Differences between the temporal or spatial estimates of FWHM were considered significant if the population differences in these values exceeded twice the population standard error.

RESULTS

Spatial Tracking System Performance

The measured and "true" absolute values of each of the six transducer coordinates determined within the sample volume were compared by linear correlation analysis. The smallest linear correlation coefficient observed in any of these comparisons was 0.9998. There was a slight tendency for the angular values to be underestimated (6% or less), but no such tendency was observed in the translational coordinates (1% or less).

FWHMs were computed in each direction for all nine point sources in each of the 45 data sets acquired with the transducer stationary within the sample volume. The population average of the X and Y FWHM values increased from anterior to posterior: X: 0.220 mm, 0.295 mm and 0.375 mm; Y: 0.254 mm, 0.302 mm and 0.352 mm. This increase was expected since points further from the transducer will move a greater distance than points near the transducer when the transducer undergoes a given angular displacement.

The average FWHM in the Z direction did not change detectably with source position, and averaged 0.202 mm. This result was also expected since the apparent Z location of a source is weakly dependent on distance from the transducer when angular motions are small, and pure Z translations affect the Z coordinates of all source points equally.

Head Movement in the Normal Subject Population

Table 1 shows population averages of the (offset-corrected) FWHM, with and without head restraint, for each source position, for each coordinate direction and for three different cumulative study intervals. We present these results in tabular form so the reader may apply a large subset of our findings to problems of his or her own design. The major trends in these results, however, are difficult to envision numerically, so we selected a representative subset of these results for graphical presentation. Accordingly, in Figure 4, population FWHMs for all three left-sided source points are plotted against time for all three coordinate directions, with and without restraint, and for two different methods of data analysis. The uncertainty (standard error) in each plotted point is also included so that the reader can judge approximately the significance of apparent differences. The shaded region of each panel contains the FWHM curves obtained by dividing the position record for each source into consecutive 5-min intervals and analyzing each of these segments as an independent data collection. The unshaded curves were obtained by dividing the position records into segments of increasing, cumulative length and computing FWHM from the data contained in each of these segments.

DISCUSSION

Head movement is a significant source of image degradation in PET (*1,2*) and other forms of tomographic brain imaging. Little, however, has been done to characterize or quantify the kind or amount of these movements under conditions typically encountered during PET brain imaging. Without such estimates, the importance of head movement as a source of image degradation in PET cannot be readily assessed nor can the efficacy of various forms of head restraint be verified. As a first step, we measured head movement in a subject group studied frequently in both the research and clinical environments, namely normal, cooperative subjects.

The Magnitude of Head Movements

Four major effects are evident in the plots shown in Figure 4 and in the data contained in Table 1. First, cumulative FWHM values increase as study length increases, with or without head restraint. Second, FWHM values computed from independent, 5-min data segments are small and nearly constant throughout the study period. Third, for the cumulative data without head restraint, X

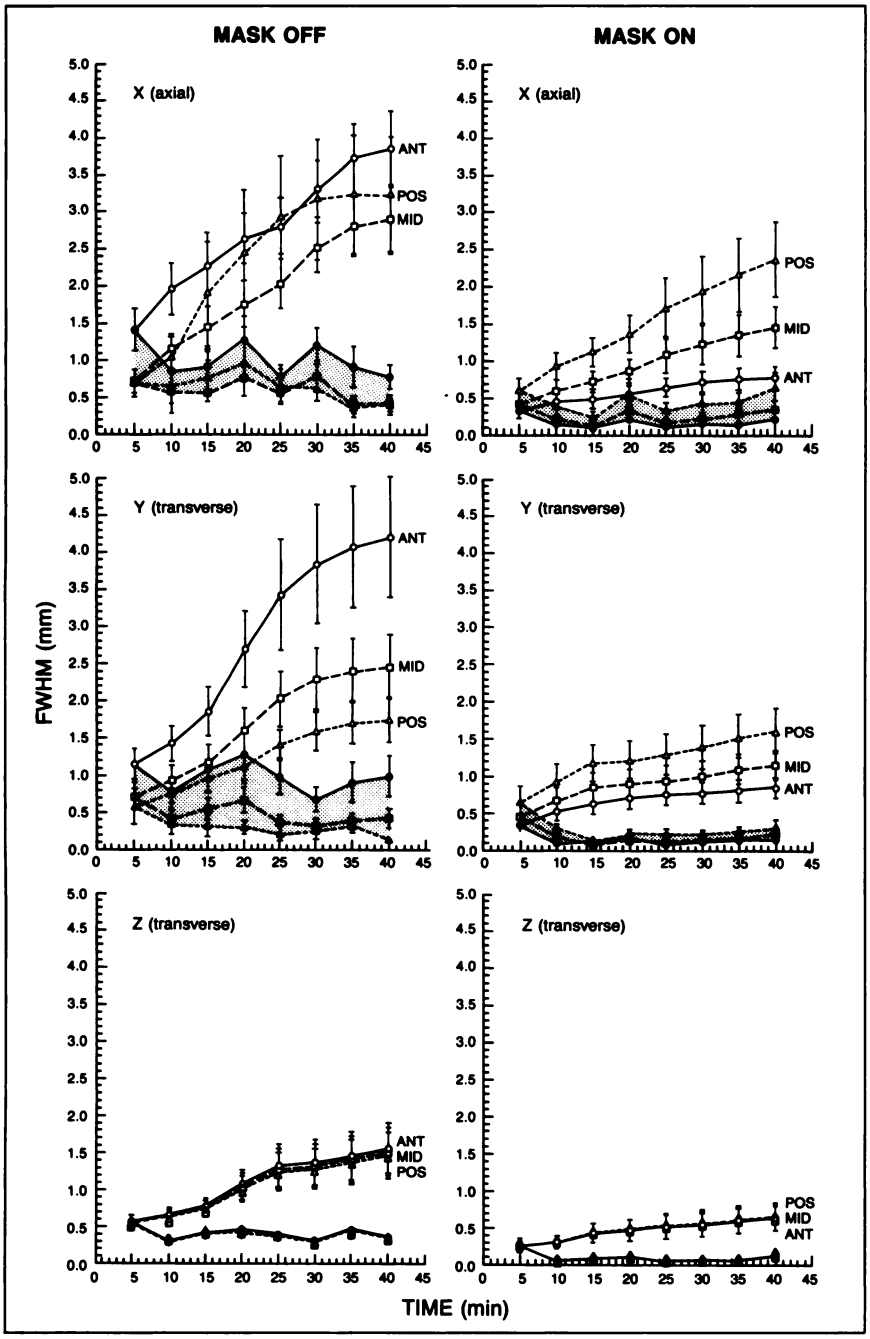

FIGURE 4. Graphs of movement FWHM in millimeters versus time in minutes for anterior (ANT), MID and posterior (POS) point sources located on the left side of the phantom head. Note that the vertical and horizontal scales in all of these graphs are identical.

and Y anterior source point movements tend to be larger than posterior source point movements. Conversely, with head restraint, posterior movements tend to be larger than anterior point source movements. This effect is most strongly evident in the cumulative Y FWHM data but is also present in the cumulative X FWHM data. The apparent difference between anterior movements with and without the mask is highly significant ($p < 0.05$). Finally, X and Y movements tend to be generally larger and the population variations greater than for the corresponding Z values.

These results support several useful generalizations. First, the magnitude of head movements in this group was small, and no population mean FWHM value exceeded 5 mm at any time, for any source, with or without head restraint. The significance of these movements in relation to the imaging process can be judged approximately by computing an "effective" spatial resolution (see Appendix E) that combines the movement FWHM with scanner FWHM according to the formula:

$$\text{FWHM(effective)} = [(\text{movement FWHM})^2 + (\text{scanner FWHM})^2]^{1/2}.$$

TABLE 1
Head Movement in Normal Volunteers*

	Time (min)	FWHM-X MASK = OFF			FWHM-X MASK = ON		
		Left	Middle	Right	Left	Middle	Right
ANT	10	2.0 (0.4)	1.7 (0.3)	1.7 (0.3)	0.5 (0.1)	0.4 (0.1)	0.5 (0.1)
	20	2.6 (0.3)	2.3 (0.4)	2.6 (0.5)	0.6 (0.1)	0.6 (0.1)	0.7 (0.1)
	40	3.9 (0.5)	2.9 (0.4)	3.0 (0.4)	0.8 (0.1)	0.7 (0.1)	0.9 (0.1)
MID							
	10	1.2 (0.1)	1.0 (0.2)	1.1 (0.3)	0.6 (0.1)	0.6 (0.1)	0.7 (0.1)
	20	1.8 (0.3)	1.7 (0.6)	2.1 (0.8)	0.9 (0.2)	0.9 (0.1)	0.9 (0.2)
	40	2.9 (0.4)	2.1 (0.5)	2.5 (0.7)	1.5 (0.3)	1.4 (0.3)	1.5 (0.4)
POS							
	10	1.1 (0.3)	1.1 (0.4)	1.4 (0.5)	0.9 (0.2)	0.9 (0.2)	0.9 (0.2)
	20	2.5 (0.8)	2.4 (1.1)	2.9 (1.4)	1.4 (0.3)	1.4 (0.3)	1.4 (0.3)
	40	3.2 (0.8)	2.7 (0.9)	3.5 (1.1)	2.4 (0.5)	2.4 (0.6)	2.5 (0.6)
ANT		FWHM-Y MASK = OFF			FWHM-Y MASK = ON		
	10	1.4 (0.2)	1.4 (0.2)	1.4 (0.2)	0.5 (0.1)	0.5 (0.1)	0.5 (0.1)
	20	2.7 (0.5)	2.7 (0.5)	2.7 (0.5)	0.7 (0.2)	0.7 (0.2)	0.7 (0.2)
	40	4.2 (0.8)	4.2 (0.8)	4.3 (0.9)	0.9 (0.1)	0.9 (0.1)	0.9 (0.1)
MID							
	10	0.9 (0.2)	0.9 (0.2)	0.9 (0.2)	0.7 (0.2)	0.7 (0.2)	0.7 (0.2)
	20	1.6 (0.3)	1.6 (0.3)	1.7 (0.3)	0.9 (0.2)	0.9 (0.2)	0.9 (0.2)
	40	2.5 (0.4)	2.5 (0.5)	2.5 (0.5)	1.2 (0.2)	1.2 (0.2)	1.2 (0.2)
POS							
	10	0.8 (0.2)	0.8 (0.2)	0.8 (0.2)	0.9 (0.2)	0.9 (0.2)	1.0 (0.2)
	20	1.1 (0.2)	1.1 (0.2)	1.1 (0.2)	1.2 (0.3)	1.2 (0.3)	1.2 (0.3)
	40	1.8 (0.3)	1.7 (0.3)	1.7 (0.3)	1.6 (0.3)	1.6 (0.3)	1.6 (0.3)
ANT		FWHM-Z MASK = OFF			FWHM-Z MASK = ON		
	10	0.7 (0.1)	0.4 (0.1)	0.7 (0.1)	0.3 (0.1)	0.1 (0.0)	0.2 (0.1)
	20	1.1 (0.2)	0.5 (0.1)	1.4 (0.2)	0.5 (0.1)	0.2 (0.1)	0.3 (0.1)
	40	1.6 (0.3)	0.7 (0.1)	2.0 (0.3)	0.7 (0.2)	0.3 (0.1)	0.4 (0.1)
MID							
	10	0.7 (0.1)	0.4 (0.1)	0.7 (0.1)	0.3 (0.1)	0.1 (0.0)	0.2 (0.1)
	20	1.1 (0.2)	0.5 (0.1)	1.4 (0.2)	0.5 (0.1)	0.2 (0.1)	0.3 (0.1)
	40	1.5 (0.3)	0.7 (0.1)	2.0 (0.4)	0.7 (0.2)	0.3 (0.1)	0.3 (0.1)
POS							
	10	0.7 (0.1)	0.4 (0.1)	0.7 (0.1)	0.3 (0.1)	0.1 (0.0)	0.2 (0.1)
	20	1.0 (0.2)	0.5 (0.1)	1.4 (0.2)	0.5 (0.1)	0.2 (0.1)	0.3 (0.1)
	40	1.5 (0.3)	0.7 (0.1)	2.0 (0.4)	0.7 (0.2)	0.3 (0.1)	0.3 (0.1)

*See Figure 2 for definition of coordinate directions and point source locations.
FWHM = movement full width at half maximum (mm) population means ± standard error.

Effective resolution computed with this equation is plotted against scanner resolution in Figure 5 for several different values of movement FWHM. The data in Table 1 can be combined with these plots to estimate the effective resolution for various combinations of movement FWHM and scanner FWHM. For example, the largest in-plane (Y-Z plane) population FWHM (at 40 min) without restraint was 4.3 mm, and with restraint was 1.6 mm. If 6 mm is taken as a typical in-plane scanner FWHM, then the corresponding effective resolutions would be 7.4 mm and 6.2 mm, respectively. Thus, a study performed in this population using a 6-mm resolution scanner could appear as much as 1.4 mm (23%) poorer without restraint, and up to 0.2 mm (3%) poorer when restraint was used. The smallest movement FWHM values occurred at the earliest times and did not exceed 1.4 mm in-plane with or without the mask. Imaging studies in this population shorter than 10-min would suffer typical resolution losses of less than 3%.

Similar calculations can be performed for axial (X) resolution. If an axial scanner resolution of 5 mm is assumed, a value consistent with contemporary PET brain scanners, Table 1 shows that the largest values for movement FWHM occur at 40 min and are 3.5 mm without restraint and 2.5 mm with restraint. The corresponding effective resolutions are 6.1 mm and 5.6 mm, respectively. Thus, axial resolution could decrease by as much as 1.1 mm (22%) without restraint and by 0.6 mm (12%) with restraint. Minimum axial movement FWHM values occurred at the earliest times and did not exceed 2 mm without restraint or 1 mm with restraint. For a 5-mm axial resolution scanner, these increases are 0.4 mm (8%) and 0.1 mm (2%), respectively. These results suggest that PET brain imaging stud-

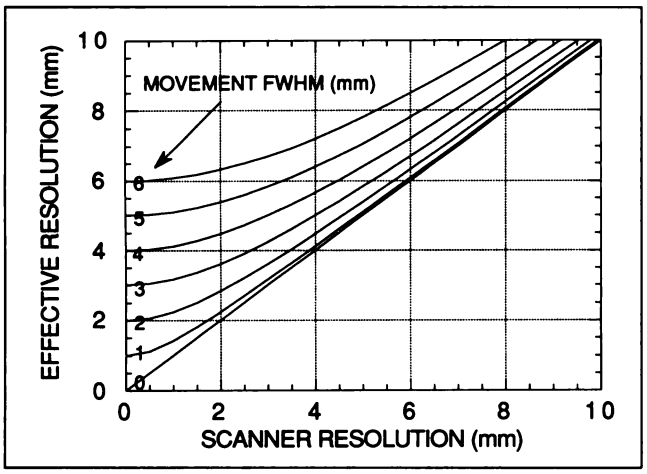

FIGURE 5. Graphical relationship between "effective" resolution and physical scanner resolution (both expressed in units of FWHM) for several different values of movement FWHM.

ies performed in normal, cooperative subjects with contemporary imaging equipment and effective head restraint, are likely to be minimally degraded by head movement.

These same movements can, however, take on substantially greater significance if movement FWHMs are comparable to physical scanner resolution. Consider, for example, a 40-min imaging study with head restraint performed using an experimental scanner with a physical resolution of 2.5 mm in all directions. According to Table 1, movement FWHMs could be as large as 2.5 mm (axial) and 1.6 mm (transverse). The corresponding effective resolutions, by Figure 5, are about 3.6 mm and 3.0 mm, giving a reduction in axial resolution of 1.1 mm (44%) and a reduction in transverse resolution of 0.5 mm (20%) compared to the design resolution. These reductions would be even greater without head restraint (Table 1) or with less effective restraint methods. Thus, as physical resolution increases, the importance of controlling head movements also increases, potentially to the point where it may be substantially more effective to focus on controlling head movements (and other second-order effects) than on improving scanner resolution.

Time Dependence of Head Movements

Figure 4 and Table 1 indicate that all cumulative movement FWHMs invariably increase with time, though not necessarily at the same rate. This increase in cumulative FWHM values is in direct contrast with the behavior of FWHM values computed when the position data records are divided into consecutive, independent 5-min intervals. Instead of rising, as do the cumulative values, sequential FWHM values remain nearly constant throughout the measurement period, and at 40 min are no larger (and in some cases actually smaller) than the initial values. Although movement FWHMs might be expected to increase with study length, such an increase could occur in at least two distinct ways: the amplitude of movements around a stable mean could increase, or the amplitude of movements around the current mean could be approximately constant but the mean position could drift with time. Figure 4 clearly indicates that in this subject population, the latter is the case and that drifts in the mean position are responsible for nearly all of the increase in cumulative FWHM with time. These results provide independent support for a simple strategy to minimize head movement artifacts, particularly in lengthy PET brain imaging studies (*1*). Instead of imaging a subject in one long data collection, the data collection is divided into a sequence of short data collections spanning the same total time interval. If the images obtained from each short data collection were spatially aligned with each other and summed, the result, according to Figure 4, would be a study minimally affected by head movement. Were this strategy perfectly implemented, its effectiveness, even for studies without restraint, could be substantial and, if applied to studies with head restraint, would virtually eliminate head movement as a source of image artifact in this study group. Although image alignment can be carried out by imaging fiducial sources placed on the head (*1*), alignment could also be carried out, at least in principle, by using the images themselves. The successful implementation of this approach, using the embedded image data for alignment, depends on the existence of alignment algorithms capable of spatially registering similar images in the presence of image "noise." Recently, several alignment algorithms have been described (*3–7*) that might prove suitable for this purpose.

Spatial Gradients in Head Movement and the Effects of Restraint

Table 1 indicates that the distribution of FWHM is not uniform over all sources. While there is no significant difference in left-right FWHM values for any source with or without the mask, there are several significant differences in FWHM between anterior and posterior sources. Without the face mask, the Y movement of anterior source points is significantly greater than the Y movement of posterior source points for all study intervals. With the face mask, as the study interval increases, the X movement of posterior source points becomes significantly greater than the X movement of anterior source points. Z movements of the sources, in contrast, with or without the mask do not exhibit such gradients, either left-right or anterior-posterior. Together, these results suggest that effective in-plane and axial spatial resolution are not uniform over the brain, but may vary spatially, depending on the kind of head restraint used, on study duration and probably on study population. In unrestrained subjects, for example, anterior in-plane structures would tend to be more blurred than posterior in-plane structures, while in restrained subjects, posterior structures would tend to be more blurred axially relative to anterior structures. While relatively small in this study, these effects could give rise to apparent differences in count density between different regions of the brain even though such differences did not actually exist. The lower anterior count density due to the gradient in unrestrained Y

movements could, for example, be interpreted as representing a biological difference in regional tracer concentration rather than as an artifact of head movement.

Significant differences in regional head movement are also present when studies with and without restraint are compared directly. The largest and most persistent of these differences is between anterior source points in the X and Y directions. These FWHM values are significantly smaller with restraint than without, even for the shortest study intervals, and grow larger with time. Other inter-study differences also exist in Table 1. Z movements of left and right source points are generally smaller with head restraint than without, though this difference does not always reach significance.

Collectively, these results suggest that the thermoplastic mask substantially reduces the ability of the head to pivot freely around a quasi-stationary point near the back of the head as it does in supine subjects without restraint. The most likely reason for this is that when the mask is properly made, the point of greatest resistance to movement is located at the bridge of the nose, a point relatively far from the pivot. By controlling roll (at the bridge of the nose) and elevation movements (with the bite plate) at some distance from the pivot, FWHM values at all points nearer to the pivot must necessarily become smaller. The inter-study difference between anterior movements introduced by the mask suggests that the particular form of head restraint used to suppress head movement may also influence the imaging process.

Data in Table 1 indicates that the mask reverses the anterior/posterior spatial gradient in FWHM observed in the unrestrained studies to such an extent as to generate a significant difference in these anterior movements. If these studies are imagined to represent two different study groups rather than the same group studied twice, one would be tempted to conclude that not only are there spatially varying differences in count density within each group, as noted above, but that there are also detectable spatial differences in count density between each group. Imagine, for example, that the no-restraint studies are typical of studies in which head movement is poorly controlled by the restraint, or in which the study population is prone to uncontrolled head movements. Imagine further that the studies with the mask represent studies in which head movements are highly constrained. If the same imaging study was now performed in these two groups, the images obtained in the group with well controlled movement would appear to possess a higher anterior count density than the group with poorly controlled movement, even if both groups were biologically identical. Thus, head-movement differences could give rise to apparent intra-group differences in regional function, even though none existed. The kind and amount of these differences could well depend on the exact movement-controlling properties of the head restraint and on the kind of patient studied.

Study Limitations

The present study is limited in several important ways. The study population consisted of cooperative, normal volunteers, all of whom were instructed to remain motionless and awake throughout the study interval and who, by observation, apparently did so. The extent to which head movements in this group resemble those in any other patient group is unknown, though it is likely that movements in these subjects are smaller than in most other patient groups. Patients undergoing real PET studies are subjected to a variety of additional conditions and stimuli that might affect head movements. For example, we did not simulate placement of the head inside an imaging gantry (see Appendix C), a situation that might increase head movement in subjects made uncomfortable by closed spaces. Instead, we concentrated on reproducing the basic geometry and body habitus most often associated with PET brain imaging and simulated only a few additional environmental factors.

The results obtained with the thermoplastic mask are also likely to be rather specific to this particular form of head restraint. The thermoplastic mask effectively suppresses anterior brain movements by preventing movement of the bridge of the nose. Restraint methods that fix other points on the head (*2*) could produce results with substantially different spatial and temporal characteristics. Nonetheless, the thermoplastic mask is used in several institutions and, at the minimum, provides a useful benchmark for other restraint methods.

Finally, the head-movement data recorded in this study were used to drive a phantom head through the same set of movements observed in each volunteer. This approach was necessary, since the exact location of the brain in each subject relative to the transducer was unknown. While the dimensions of this phantom head and the placement of sources within the head were selected based on adult head/brain atlas measurements and on measurements made in normal subjects, some differences must exist between this phantom and the individuals studied. The net result of such differences is that the embedded source points might not correspond exactly to the same anatomical structures in each subject. Movement of the point sources might thus under- or overestimate the movement of specific brain structures in individual subjects. In our view, such departures are likely to be small since the dimensions of the adult human head do not vary greatly and since these movement data were averaged over the whole population.

CONCLUSION

Without restraint, head movement in a population of normal, cooperative supine subjects increases with study duration. Head movements also increase with time when a thermoplastic mask is used to restrict these movements, but the rate of increase and the magnitude of increase are much smaller than without the mask. Spatial gradients in head movement also appear to exist with or without restraint, but the pattern of these gradients is different for the

two conditions often by a factor of 2 or more. This result suggests that different methods of head restraint, or different movement patterns in different patient populations, could introduce systematic and artifactual differences into images obtained in these groups. The appearance of nonbiological differences, moreover, could be exacerbated through the use of analytic methods particularly sensitive to such differences. However, if all studies were performed with the restraint used here (or its equivalent), movements would be reduced to a level where image quality would not be significantly compromised except at the highest resolutions attainable with PET.

Finally, these data support the use of a potentially simple technique for reducing the effects of head movement: segmenting data collection into a sequence of short images, spatially aligning these images and then summing them together. The resulting image should be largely unaffected by head movement regardless of the length of the imaging interval.

APPENDIX

A. Spatial position and orientation were measured with a Polhemus Navigation Sciences 3Space Tracker (Model 002). The 3Space Tracker product is no longer available, but information about functionally similar units can be obtained from: Polhemus, P.O. Box 560, 1 Hercules Dr., Colchester, VT 05446

B. The particular thermoplastic mask/head support system described in this work was fabricated and tested at the NIH and was based on a design believed to have originated at Washington University in St. Louis, MO. Information about a similar, commercially available restraint system can be obtained from: Tru-Scan Imaging, (Patient Immobilizers), P.O. Box 404, Annapolis, MD 21404

C. The accuracy of the tracking system was evaluated in an actual PET (brain) scanner (Scanditronix/GE PC2048-15B) by rotating and translating the transducer through known displacements within the scanning aperture. The device performed poorly (inaccurately) in this setting due, presumably, to the distribution of metal around the aperture in relation to the transducer/reference source combination.

D. Assume that a point source is located at y, z in a plane fixed in, and moving with, the patient's head. Assume also that the location of this same point in the (stationary) reference source coordinate system is given by X, Y, Z and that the location of the center of the transducer in this stationary system is given by X_o, Y_o, Z_o. If C and S represent the cosine and sine functions, respectively, and A, E and R represent the azimuth, elevation and roll angles of the transducer, respectively, then y and z are related to X, Y and Z by the equations:

$$X = X_o + y\,[(CA)(SE)(SR) - (SA)(CR)] + z\,[(CA)(SE)(CR) + (SA)(SR)],$$

$$Y = Y_o + y\,[(CA)(CR) + (SA)(SE)(SR)] + z\,[(SA)(SE)(CR) - (CA)(SR)],$$

$$Z = Z_o + y\,[(CE)(SR)] + z\,[(CE)(CR)],$$

where CA = cosine (azimuth), SE = sine (elevation), etc. For each data sample, the six acquired coordinates are inserted into these equations and the new position of each point source in the stationary coordinate system is computed and stored. The record of these transformed positions for all nine sources in the three coordinate directions is then analyzed to estimate the variance (or movement FWHM) associated with each source in each direction.

E. Results in this study were expressed as FWHM by multiplying a given standard deviation by the factor 2.35, the factor that transforms a Gaussian standard deviation into a Gaussian FWHM. This scaling was performed only as a convenience to the reader so that these values might be more easily compared to a quantity of familiar magnitude, namely scanner resolution expressed as FWHM. The use of the term "FWHM" is not meant to imply that the distribution functions underlying the head position measurements were necessarily Gaussian (they were not), nor that the quadrature combination (*8*) of scanner and movement FWHM yields another Gaussian distribution (it does not). It is, however, useful to think of these variables as emanating from "effective" Gaussian distributions as an aid to visualizing and interpreting the results. We carried out this scaling transformation for this reason.

REFERENCES

1. Koeppe RA, Holthoff VA, Frey KA, et al. Compartmental analysis of 11-C Flumazenil kinetics for the estimation of ligand transport rate and receptor distribution using positron emission tomography. *J Cereb Blood Flow Metab* 1991;11:735–744.
2. Bergstrom M, Boethius J, Eriksson L, et al. Head fixation device for reproducible position alignment in transmission CT and positron emission tomography. *J Comput Assist Tomogr* 1981;5:136–141.
3. Phillips RL, London ED, Links JM, et al. Program for PET image alignment: effects on calculated differences in cerebral metabolic rates for glucose. *J Nucl Med* 1990;31:2052–2057.
4. Minoshima S, Berger KL, Lee KS, et al. An automated method for rotational correction and centering of three-dimensional functional brain images. *J Nucl Med* 1992;33:1579–1585.
5. Junck L, Moen JG, Hutchins GD, et al. Correlation methods for the centering, rotation and alignment of functional brain images. *J Nucl Med* 1990;31:1220–1276.
6. Alpert NM, Bradshaw JF, Kennedy D, et al. The principal axes transformation: a method for image registration. *J Nucl Med* 1990;31:1717–1722.
7. Woods RP, Cherry SR, Mazziotta JC. Rapid automated algorithm for aligning and reslicing PET images. *J Comput Assist Tomogr* 1992;16:620–633.
8. Raeside, DE. Probability and statistics. In: Morin RL, ed. *Monte Carlo simulation in the radiological sciences.* Boca Raton: CRC Press; 1988:30–35.